International Journal of Robotics and Automation, Vol. 36, 2021

Special Issue: Artificial Intelligence in Environmental Automation Systems

BACK-PROPAGATION NEURAL NETWORK–BASED MODELLING FOR SOIL HEAVY METAL

Fang Li,*,** Anxiang Lu,** Jihua Wang,** and Tianyan You*

Abstract

X-ray fluorescence (XRF) technology is a widely used method for rapid detection of heavy metals in soil. It is important to establish accurate models of the XRF spectrometer. Firstly, the influence of sample particle size on the detection results was investigated, and the 100 mesh was the most suitable particle size. All spectra were pre-processed before modelling using the Savitzky–Golay smoothing with seven points and the wavelet transform method with Coif 3 wavelet base at the ninth level for noise deduction and baseline correction. The error back-propagation artificial neural network (BP-ANN) learning algorithm optimized by Levenberg–Marquart (LM) algorithm was selected to establish soil heavy metal models. The results indicated that the modelling results were sufficiently accurate. The BP-ANN method optimized with LM algorithm was applied in the XRF research field for the first time, which provides some technical support for the establishment of rapid detection models of heavy metals in soil.

Key Words

Levenberg–Marquart, back-propagation neural network, soil, heavy metal

1. Introduction

Heavy metals are particularly prominent among soil inorganic pollutants, mainly because heavy metals cannot be decomposed by soil micro-organisms and are easy to accumulate [1], [2]. They can be converted into more toxic methyl compounds, and some even accumulate in the human body in harmful concentrations through the food chain, seriously endangering human health [3]–[5]. Therefore, the detection of heavy metals in farmland soil, especially rapid detection, is particularly important. In this study, we will focus on some heavy metals that have caused widespread concern about soil toxicity, including As, Cr, Cu, Pb and Zn (As is considered a metalloid).

X-ray fluorescence (XRF) analysis is widely used in heavy metal detection in soil because it is non-destructive, simple to operate, low cost and fast detection [6], [7]. XRF analysis can be used to identify specific elements in substances and quantify them at the same time. It can determine the specific element according to the emission wavelength and energy of the X-ray, and determine the content of this element by measuring the density of the corresponding ray [8], [9]. Many studies focused on the application of portable XRF spectrometer to detect heavy metals in soil [10]–[20]. Few researches have discussed XRF spectral data processing, analysis and modelling. The reason may be that most users of XRF spectrometer do not have the ability to manufacture the instrument, and it is a rather complicated work to study the modelling method, so most studies only pay attention to the application of XRF spectrometer. In this work, the error back-propagation artificial neural network (BP-ANN) learning algorithm optimized by Levenberg–Marquart (LM) algorithm was used to establish accurate XRF quantitative detection models of soil heavy metals.

2. Materials and Methods

2.1 Collection of Soil Samples, Apparatus and Detection Conditions

The soil samples were collected from 0 to 20 cm surface soil in various fields and mining areas. Before detection, all samples were simply processed indoors, including air-dried, ground and sieved. Non-metallic tools were used throughout the process to prevent the introduction of metals.

All detections were performed with a portable XRF spectrometer (NX-100S, NCS Testing Technology Co., Beijing, China) fitted with a W anode X-ray tube, Cu filter and silicon drift detector. The apparatus was operated at a voltage of 38 kV, current of 120 μA and detection time of 240 s. An ethylene sample cup ($D \times H$: 25 mm × 40 mm, NCS Testing Technology Co., Beijing, China) fixed with a Mylar film (Premier Lab Supply Co., Woburn, MA, USA;

* School of Agricultural Engineering, Institute of Agricultural Engineering, Jiangsu University, Zhenjiang, Jiangsu 212013, China; e-mail: {viki2069, youtyujs}@126.com

** Beijing Research Center for Agricultural Standards and Testing, Beijing 100097, China; e-mail: {anxxlu, jhwangatfm}@163.com

Corresponding author: Tianyan You

Recommended by Dr. Dong Ren

(DOI: 10.2316/J.2021.206-0618)

special film for X-ray analysis, thickness: 6 μm) was used to place the samples. Each sample was detected seven times, and the average spectrum was calculated for subsequent analysis. Corresponding chemical values of heavy metals in all samples were detected by national standard methods, and a national standard soil sample was added for quality control.

2.2 Sample Detection Conditions

The state of the sample has a certain impact on the detection results. When soil heavy metals are detected, the most influential factors include water content and particle size. In this study, the soil samples were air-dried indoor to keep the water content lower than 5%. To determine the suitable particle size, some ground and sieved samples were detected after passing through 10 mesh, 18 mesh, 40 mesh, 60 mesh, 80 mesh, 100 mesh and 120 mesh screen.

2.3 Pre-processing Methods of the X-ray Fluorescence Spectra

The XRF spectra contain both useful chemical information and interference information such as background noise and irrelevant information. These interference factors have great influence on the extraction of target spectral information [21]. Therefore, it is necessary to pre-process the spectra to establish accurate quantitative detection models, and improve the robustness and prediction accuracy of the model.

Savitzky–Golay (SG) smoothing is a spectral pre-processing method that can effectively eliminate noise such as baseline drift and tilt [22], [23]. The parameters of SG include derivative order, polynomial order and smoothing point, and the number of smoothing point is an important parameter. Too few smoothing points can easily generate new calculation errors, which will reduce the accuracy of the model. Too many smoothing points will make the spectral data lost sample information and reduce the accuracy of the model. Therefore, an accurate quantitative detection model can be established by determining the appropriate number of smoothing points [24]–[26]. Wavelet transform (WT) is a new branch of mathematics, it is the perfect combination of functional, Fourier analysis, harmonic analysis and numerical analysis [27], [28]. In the application field, especially in signal processing, image processing, speech processing and many non-linear science fields, it is considered to be another effective time-frequency analysis method after Fourier analysis [29]. Compared with the Fourier transform, the WT is a local transform in the time and frequency domains, which can effectively extract information from the signal, and perform multi-scale analysis on the function or signal through operation functions such as scaling and translation[30]–[32].

2.4 Establishment of Quantitative Detection Model for Heavy Metals in Soil

The accuracy of the quantitative detection models will be affected by different modelling methods. ANN is a common method for analysing metrology problems. It is usually used to solve complex problems, such as some uncertain non-linear relationship problems [33]. The method has been widely used in many fields because the established model has high accuracy, strong anti-interference, and strong classification and prediction ability. The error BP-ANN algorithm is the most widely used learning algorithm in the ANN model. BP-ANN is a supervised learning algorithm, which is mainly composed of forward propagation of information and backward propagation of error [34]. The learning process is a process of repeated alternation. The gradient adjustment error is used to change the weights and thresholds of the neural network until the network convergence is reached [35]–[37].

3. Results and Discussion

3.1 Particle Size of Detected Samples

Few attentions had been paid to the effect of sample size on the detection results in XRF analysis. In this study, samples with different particle size were detected to determine a suitable particle size for accurate results. Samples were protected from light and sealed after sieving with 10 mesh, 18 mesh, 40 mesh, 60 mesh, 80 mesh, 100 mesh and 120 mesh screen. Parallel detection was performed seven times and the relative standard deviation (RSD) was calculated to examine the precision (Fig. 1). When the particle size of the sample is <100 mesh, the RSD decreases as the particle size decreases. When the particle size of the sample is >100 mesh, RSD tends to be stable; there is no significant difference between the 100 mesh and 120 mesh samples. Through comprehensive comparison, the 100 mesh particle size was selected for subsequent experiments.

3.2 Spectral Pre-processing Results

All spectral pre-processing were performed on MATLAB version 2014a software (MathWorks Inc., Natick, MA, USA). All programs were written locally in the lab. The SG smoothing with seven points was used followed by the WT method with Coif 3 wavelet base at the ninth level for noise deduction and baseline correction. Adaptive threshold was used in denoising by WT decomposition, which regard per scale level as an independent part. Three directions are decomposed at each level according to the different characteristics of the wavelet coefficients amplitude, including the horizontal direction, vertical direction and diagonal direction. A threshold that best matches each direction is found for denoising, so that the noise in all directions can be separated. The pre-processing result (Fig. 2) indicted that the effective information of the characteristic peaks was well preserved while the noise and background were removed.

3.3 Comparison of Different Modelling Methods

The disadvantage of BP-ANN is that the approximation process takes a long time, the local minimum value is often

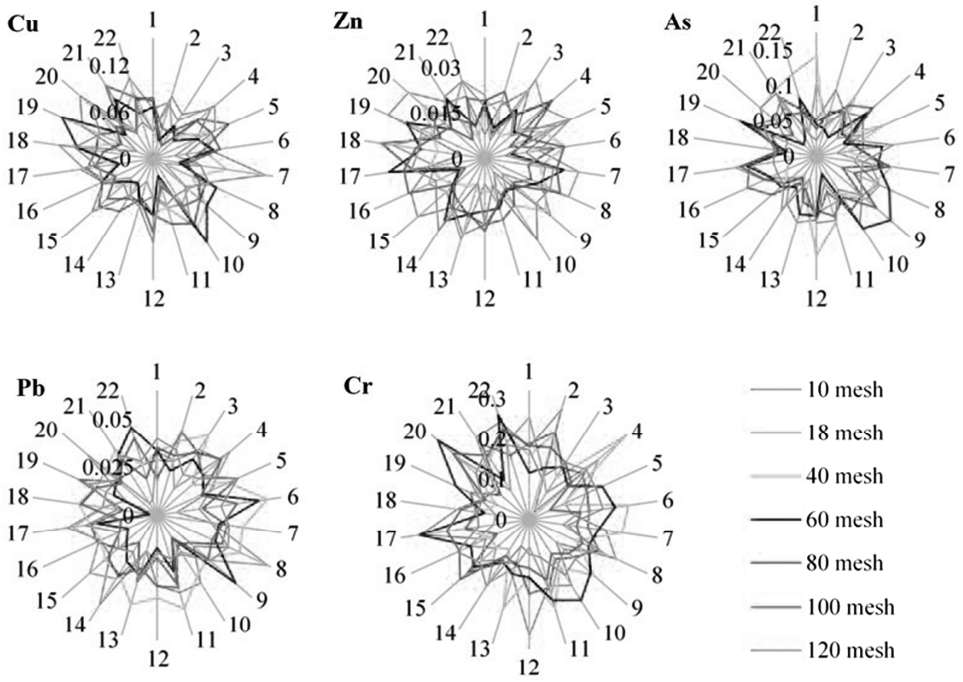

Figure 1. RSD of soil samples with different particle sizes.

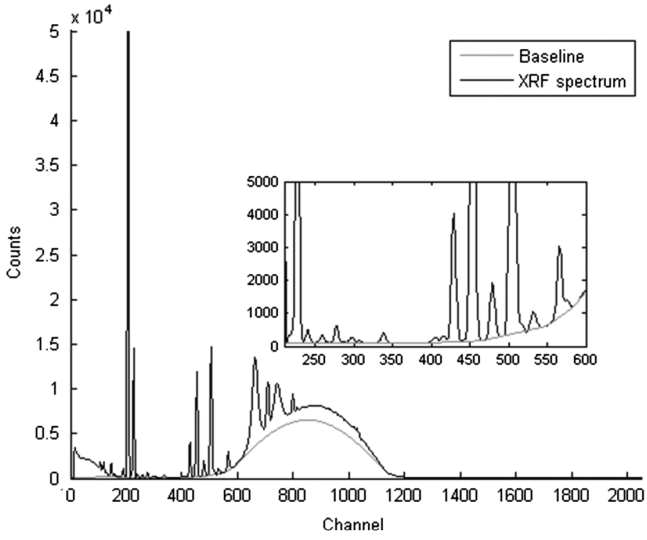

Figure 2. Pre-processing results of XRF spectra using SG smoothing and WT method.

Table 1
Modelling Results by Different Regression Methods

Modelling Method	Evaluation Index	Cr	Cu	Zn	As	Pb
PR	r^2	0.990	0.992	0.991	0.992	0.996
BPR		0.991	0.989	0.990	0.983	0.989
LM-BPR		0.994	0.996	0.995	0.994	0.997
SVMR		0.954	0.962	0.968	0.966	0.964
PLSR		0.968	0.991	0.970	0.979	0.985
PR	MSE	27.89	18.35	24.39	13.81	16.25
BPR		37.34	30.61	45.37	42.32	24.29
LM-BPR		15.70	10.55	12.78	19.61	14.43
SVMR		22.84	23.57	42.17	24.36	32.87
PLSR		33.61	25.15	56.24	40.73	21.67

wrongly taken as the result, the data fluctuates greatly and it is difficult to obtain appropriate model parameters. Therefore, it is less likely to use BP-ANN to obtain the global optimal solution, which limits its use. In this study, the LM algorithm was used to optimize BP-ANN. The LM algorithm is a synthesis of Gauss–Newton method and steepest descent method. LM has the advantages of local convergence of the former and global characteristics of the latter [38]. The self-adaptability of LM makes it possible to adjust the damping factor to obtain the results, so the iteration convergence speed becomes faster, and stable and reliable solutions are obtained in many non-linear optimization problems [39]–[43]. Compared with ordinary BP algorithm, LM-BP has fewer iterations, faster convergence and higher accuracy, and is not easy to converge to local extremum.

Different modelling methods were used to build the quantitative detection models of heavy metals in soil samples, including polynomial regression (PR), BP-ANN regression (BPR), LM-BP-ANN regression (LM-BPR), support vector machine regression (SVMR) and partial least squares regression (PLSR). The mean square error (MSE) and decision coefficient (r^2) were used to evaluate the accuracy of the modelling results. The modelling results (Table 1) showed that with the LM-BPR method,

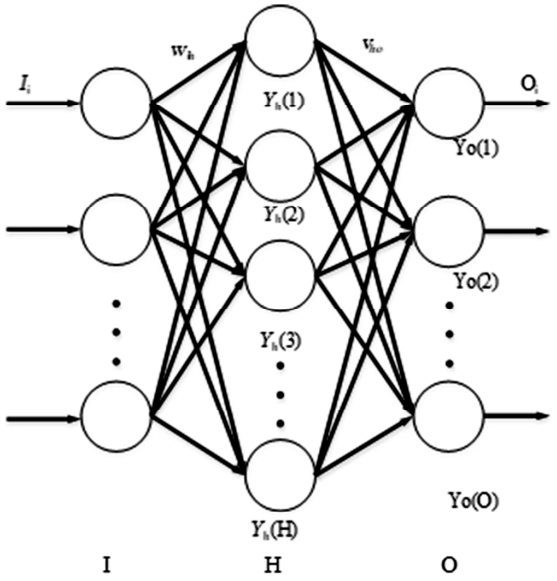

Figure 3. Structure of a typical three-layer BP-ANN.

all of the r^2 of five heavy metals were the highest, and the MSE values were the lowest (except for As, which got the lowest MSE with the PR method). Therefore, LM-BPR was chosen as the modelling method because it has better accuracy.

3.4 Modelling Results by LM-BPR

Before modelling, the concentration gradient method was used to divide the sample data into three parts: training set, validation set and test set with a ratio of 2:1:1. The function of training set is to establish the calibration model, and the validation set and the test set are used to assess the model. The input of the model is the sample spectral of the training set, and the corresponding target element contents of the training set sample were used as the expected output matrix. A typical three-layer BP-ANN was used to train and establish the quantitative analysis model, including the input layer (I), the output layer (O) and the hidden layer (H) (Fig. 3).

The signal I_i is written, assigned weight and normalized by the input layer, and then the data is sent to the hidden layer, where the data is calculated and analysed according to the previously assigned weight. The obtained result is transferred to the output layer to get the output signal O_i through non-linear transformation. The sample in the training network is composed of the input vector (I), the expected output value (T), the network output value (O) and the deviation of T. The error is reduced according to the gradient direction by adjusting the network weight w_{ih} between the input layer node and the hidden layer node, the network weight v_{ho} between the hidden layer node and the output layer node, and the threshold value. By repeating this process, the weights and thresholds are obtained at the lowest error level. The successful modelling neural network can present the calculation results with the smallest output error with nonlinear processing.

Table 2
Optimization Conditions of BP-ANN for Different Heavy Metals

	Cr	Cu	Zn	As	Pb
Neurons number	4	3	7	5	4
Learning rate	0.3	0.25	0.2	0.2	0.05
Epoch time	11	6	8	15	40

Table 3
Decision Coefficient (r^2) of Modelling Results for Different Data Set

	r^2_{train}	r^2_{valid}	r^2_{test}	r^2_{whole}
Cr	0.9986	0.9934	0.9919	0.9942
Cu	0.9996	0.9937	0.9880	0.9955
Zn	0.9998	0.9959	0.9808	0.9946
As	0.9986	0.9922	0.9900	0.9943
Pb	0.9998	0.9938	0.9942	0.9968

Optimization conditions were required for modelling, including the number of hidden layer neurons, learning rate and epoch time. The number of neurons in the hidden layer affects the prediction accuracy. Too few hidden layer neurons will result in too simple results and insufficient prediction accuracy. Too many neurons will lead to overfitting and inaccurate prediction results. The number of neurons in the hidden layer was measured in the range of 3–20 in this study. The learning rate affects the speed of the processing. Too low learning rate can easily lead to slow processing speed, long training cycle, and slow convergence speed; too high learning rate can easily cause system instability, resulting in data fluctuations and data redundancy. The best learning rate was optimized in the range of 0.05–0.8. In the experimental results, the MSE between the predicted results and the actual value was taken as the evaluation index and the smaller the value, the better the result. The optimized parameters are presented in Table 2.

Quantitative soil heavy metal analysis models of training set, validation set, test set and whole data set were established after the spectra were pre-processed. The decision coefficient of the training set (r^2_{train}), validation set (r^2_{valid}), test set (r^2_{test}) and the whole data set (r^2_{whole}) between the model prediction results and the standard values (detected by corresponding chemical analysis method) is presented in Table 3. The modelling results (Fig. 4) showed that the values were numerically close, indicating that the results predicted by LM-BPR were sufficiently accurate.

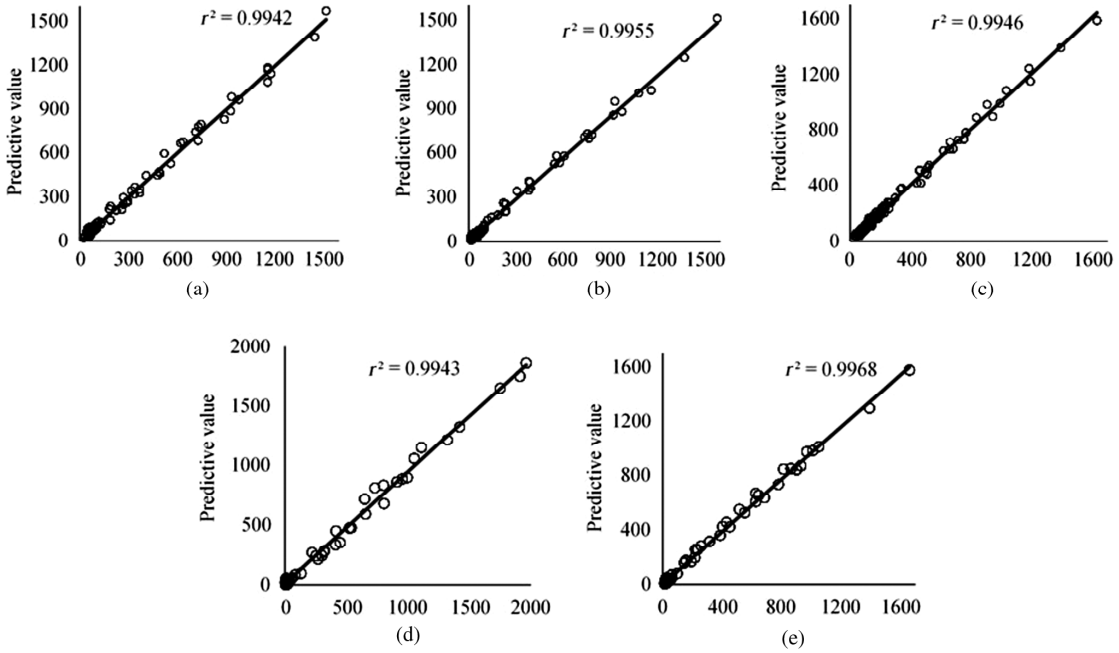

Figure 4. Correlation between standard value (chemical analysis) and predicted value (XRF modelling results) for Cr (a), Cu (b), Zn (c), As (d) and Pb (e) on the whole data set.

4. Conclusion

The detection conditions were optimized and the optimum particle size was determined to be 100 mesh. Accurate quantitative models for Cr, Cu, Zn, As and Pb were built using LM-BPR method on the basis of the pre-processing method with SG smoothing and WT analysis. The advantages of LM-BPR method are small matrix effect, convenient calculation and high reliability of quantitative detection. Several modelling methods were compared, the LM-BPR showed higher accuracy than other methods. The LM-BPR method has high modelling efficiency and good stability, and can effectively avoid local convergence. By using the LM-BPR method, a rapid quantitative analysis method was established by building different heavy metal models separately, which provides some theoretical support for using XRF spectrometer to improve the rapid and accurate detection of heavy metals in soil.

Acknowledgement

This study was supported by the National Key Research and Development Program of China (Grant No. 2016YFD0800902). We would like to thank the editors and reviewers for their valuable comments and suggestions.

References

[1] Z. Li, Z. Ma, T.J. van der Kuijp, Z. Yuan Z, and L. Huang, A review of soil heavy metal pollution from mines in China: Pollution and health risk assessment, *Science of the Total Environment*, *468–469*, 2014, 843–853.

[2] S. Khalid, M. Shahid, N.K. Niazi, B. Murtaza, I. Bibi, and C. Dumat, A comparison of technologies for remediation of heavy metal contaminated soils, *Journal of Geochemical Exploration*, *182*, 2017, 247–268.

[3] H. Chen, Y. Teng, S. Lu, Y. Wang, and J. Wang, Contamination features and health risk of soil heavy metals in China, *Science of the Total Environment*, *512–513*, 2015, 143–153.

[4] Q. Duan, J. Lee, Y. Liu, H. Chen, and H. Hu, Distribution of heavy metal pollution in surface soil samples in China: A graphical review, *Bulletin of environmental contamination and toxicology*, *97*(3), 2016, 303–309.

[5] K.S. Balkhair and M.A. Ashraf, Field accumulation risks of heavy metals in soil and vegetable crop irrigated with sewage water in western region of Saudi Arabia, *Saudi Journal of Biological Sciences*, *23*(1), 2016, S32–S44.

[6] T. Radu and D. Diamond, Comparison of soil pollution concentrations determined using AAS and portable XRF techniques, *Journal of Hazardous Materials*, *171*(1–3), 2009, 1168–1171.

[7] B. Song, G. Zeng, J. Gong, J. Liang, P. Xu, Z. Liu, *et al.*, Evaluation methods for assessing effectiveness of in situ remediation of soil and sediment contaminated with organic pollutants and heavy metals, *Environment International*, *105*, 2017, 43–55.

[8] H. Rowe, N. Hughes, and K. Robinson, The quantification and application of handheld energy-dispersive x-ray fluorescence (ED-XRF) in mudrock chemostratigraphy and geochemistry, *Chemical Geology*, *324–325*, 2012, 122–131.

[9] A. Turner, H. Poon, A. Taylor, and M.T. Brown, In situ determination of trace elements in *Fucus* spp. by field-portable-XRF, *Science of the Total Environment*, *593–594*, 2017, 227–235.

[10] E.L. Shuttleworth, M.G. Evans, S.M. Hutchinson, and J.J. Rothwell, Assessment of lead contamination in peatlands using field portable XRF, *Water, Air, & Soil Pollution*, *225*(2), 2014, 1844–1856.

[11] N.G. Paltridge, L.J. Palmer, P.J. Milham, G.E. Guild, and J.C.R. Stangoulis, Energy-dispersive X-ray fluorescence analysis of zinc and iron concentration in rice and pearl millet grain, *Plant and Soil*, *361*(1–2), 2012, 251–260.

[12] W. Hu, B. Huang, D.C. Weindorf, and Y. Chen, Metals analysis of agricultural soils via portable X-ray fluorescence spectrometry, *Bulletin of Environmental Contamination and Toxicology*, *92*(4), 2014, 420–426.

[13] A.G. Caporale, P. Adamo, F. Capozzi, G. Langella, F. Terribile, and S. Vingiani, Monitoring metal pollution in soils using portable-XRF and conventional laboratory-based techniques: Evaluation of the performance and limitations according to metal properties and sources, *Science of the Total Environment*, *643*, 2018, 516–526.

[14] A. Chandrasekaran, R. Ravisankar, N. Harikrishnan, K.K. Satapathy, M.V. Prasad, and K.V. Kanagasabapathy, Multivariate statistical analysis of heavy metal concentration in soils of Yelagiri Hills, Tamilnadu, India – spectroscopical approach,

Spectrochimica Acta Part A: Molecular and Biomolecular Spectroscopy, *137*, 2015, 589–600.
[15] A. Turner and A. Taylor, On site determination of trace metals in estuarine sediments by field-portable-XRF, *Talanta*, *190*, 2018, 498–506.
[16] S. Chakraborty, T. Man, L. Paulette, S. Deb, B. Li, D.C. Weindorf, *et al.*, Rapid assessment of smelter/mining soil contamination via portable X-ray fluorescence spectrometry and indicator kriging, *Geoderma*, *306*, 2017, 108–119.
[17] S. Zhou, Z. Yuan, Q. Cheng, Z. Zhang, and J. Yang, Rapid in situ determination of heavy metal concentrations in polluted water via portable XRF: Using Cu and Pb as example, *Environmental Pollution*, *243*(Pt B), 2018, 1325–1333.
[18] B. Lemière, A review of pXRF (field portable X-ray fluorescence) applications for applied geochemistry, *Journal of Geochemical Exploration*, *188*, 2018, 350–363.
[19] M. Qu, Y. Wang, B. Huang, and Y. Zhao, Spatial uncertainty assessment of the environmental risk of soil copper using auxiliary portable X-ray fluorescence spectrometry data and soil pH, *Environmental Pollution*, *240*, 2018, 184–190.
[20] E.O. Kazimoto, C. Messo, F. Magidanga, and E. Bundala, The use of portable X-ray spectrometer in monitoring anthropogenic toxic metals pollution in soils and sediments of urban environment of Dar es Salaam Tanzania, *Journal of Geochemical Exploration*, *186*, 2018, 100–113.
[21] V.A. Solé, E. Papillon, M. Cotte, P. Walter, and J. Susini, A multiplatform code for the analysis of energy-dispersive X-ray fluorescence spectra, *Spectrochimica Acta Part B: Atomic Spectroscopy*, *62*(1), 2007, 63–68.
[22] M.U.A. Bromba and H. Ziegler, Application hints for Savitzky–Golay digital smoothing filters, *Analytical Chemistry*, *53*(11), 1981, 1583–1586.
[23] R.W. Schafer, What is a Savitzky–Golay filter?, *IEEE Signal Processing Magazine*, *28*(4), 2011, 111–117.
[24] D. Acharya, A. Rani, S. Agarwal, and V. Singh, Application of adaptive Savitzky–Golay filter for EEG signal processing, *Perspectives in Science*, *8*, 2016, 677–679.
[25] Y. Liu, B. Dang, Y. Li, H. Lin, and H. Ma, Applications of Savitzky–Golay filter for seismic random noise reduction, *Acta Geophysica*, *64*(1), 2016, 101–124.
[26] G. Vivó-Truyols and P.J. Schoenmakers, Automatic selection of optimal Savitzky–Golay smoothing, *Analytical Chemistry*, *78*(13), 2006, 4598–4608.
[27] D. Gupta and S. Choubey, Discrete wavelet transform for image processing, *International Journal of Emerging Technology and Advanced Engineering*, *4*(3), 2015, 598–602.
[28] C. Ma, J. Li, and D. Wang, Optimal evaluation index system and benefit evaluation model for agricultural informatization in Beijing, *International Journal of Robotics and Automation*, *33*(1), 2018, 89–96.
[29] A. Bhattacharyya, M. Sharma, R.B. Pachori, P. Sircar, and U.R. Acharya, A novel approach for automated detection of focal EEG signals using empirical wavelet transform, *Neural Computing and Applications*, *29*(8), 2016, 47–57.
[30] D. De Yong, S. Bhowmik, and F. Magnago, An effective power quality classifier using wavelet transform and support vector machines, *Expert Systems with Applications*, *42*(15–16), 2015, 6075–6081.
[31] Z. Lai, X. Qu, Y. Liu, D. Guo, J. Ye, Z. Zhan, *et al.*, Image reconstruction of compressed sensing MRI using graph-based redundant wavelet transform, *Medical Image Analysis*, *27*, 2016, 93–104.
[32] A. Bhattacharyya, R. Pachori, A. Upadhyay, and U. Acharya, Tunable-Q wavelet transform based multiscale entropy measure for automated classification of epileptic EEG signals, *Applied Sciences*, *7*(4), 2017, 385–402.
[33] M. Hemmat Esfe, M.R. Hassani Ahangar, M. Rejvani, D. Toghraie, and M.H. Hajmohammad, Designing an artificial neural network to predict dynamic viscosity of aqueous nanofluid of TiO_2 using experimental data, *International Communications in Heat and Mass Transfer*, *75*, 2016, 192–196.
[34] S. Shi, D. Zhang, P. Feng, and L. Han, The enhancement arithmetic of BP neural network based on target optimizing, *2018 International Conference on Computer Modeling, Simulation and Algorithm (CMSA 2018)*, (Beijing, China: Atlantis Press, 2018), *151*, 2018, 137–141.
[35] Q.G. Wen, K.F. Sun, and H. Yen, A method of temperature prediction and velocity control based on BP artificial neural network, *2016 International Conference on Information System and Artificial Intelligence (ISAI) IEEE*, Hong Kong, China, 2016, 327–331.
[36] G.-Z. Quan, Z.-H. Zhang, J. Pan, and Y.-F. Xia, Modelling the hot flow behaviors of AZ80 alloy by BP-ANN and the applications in accuracy improvement of computations, *Materials Research*, *18*(6), 2015, 1331–1345.
[37] C. Yang, Z. Wang, L. Zheng, and D. Mao, Predicting equivalent static density of fuzzy ball drilling fluid by BP artificial neutral network, *Advances in Materials Science and Engineering*, *2015*, 2015, 1–6.
[38] S. Mammadli, Financial time series prediction using artificial neural network based on Levenberg–Marquardt algorithm, *Procedia Computer Science*, *120*, 2017, 602–607.
[39] M.G. Shirangi and A.A. Emerick, An improved TSVD-based Levenberg–Marquardt algorithm for history matching and comparison with Gauss–Newton, *Journal of Petroleum Science and Engineering*, *143*, 2016, 258–271.
[40] A. Gholami, F. Honarvar, and H.A. Moghaddam, Modeling the ultrasonic testing echoes by a combination of particle swarm optimization and Levenberg–Marquardt algorithms, *Measurement Science and Technology*, *28*(6), 2017, 065001.
[41] Ö. Çelik, A. Teke, and H.B. Yıldırım, The optimized artificial neural network model with Levenberg–Marquardt algorithm for global solar radiation estimation in Eastern Mediterranean Region of Turkey, *Journal of Cleaner Production*, *116*, 2016, 1–12.
[42] J. Li, W.X. Zheng, J. Gu, and L. Hua, Parameter estimation algorithms for Hammerstein output error systems using Levenberg–Marquardt optimization method with varying interval measurements, *Journal of the Franklin Institute*, *354*(1), 2017, 316–331.
[43] M. Kayri, Predictive abilities of Bayesian regularization and Levenberg–Marquardt algorithms in artificial neural networks: A comparative empirical study on social data, *Mathematical and Computational Applications*, *21*(2), 2016, 20–30.

Biographies

Fang Li graduated from Jilin University (China) with an MA.Eng at Agricultural Engineering in 2015. She is currently a Ph.D. candidate in Agricultural Engineering at Jiangsu University, Zhenjiang, China. Her current research focuses on X-ray fluorescence spectra analysis and the establishment of accurate quantitative models of soil heavy metals.

Anxiang Lu is a Professor of Beijing Research Center for Agricultural Standards and Testing. He received his Ph.D. degree in Environmental Science at Chinese Academy of Sciences (Beijing, China), in 2011. He has published about 30 scientific peer-reviewed papers. His current research activities include farmland environmental monitoring, multivariate calibration and regression methods.

Jihua Wang is a Professor of Beijing Research Center for Agricultural Standards and Testing. He received his Ph.D. degree at China Agricultural University, Beijing, China. He is Chinese agricultural product quality and safety expert, and national agricultural information expert. He has coauthored more than 70 peer-reviewed papers. He has directed about 30 doctoral thesis. His actual research focuses on remote sensing, agricultural information and IOT technology.

Tianyan You is a Professor of Jiangsu University, Zhenjiang, China. She received her Ph.D. degree at Chinese Academy of Sciences (Changchun, China), in 1999. She has published more than 100 peer-reviewed papers. Her research expertise focuses on environmental pollutant analysis, electrochemical biosensor research and modern agricultural sensing.